Effects of Interfacial Instability on Film Boiling of Saturated Liquid Helium I Above a Horizontal Surface

T. H. K. FREDERKING, Y. C. WU, and B. W. CLEMENT

University of California, Los Angeles, California

Film boiling above a horizontal surface has been investigated theoretically and experimentally at standard gravity and 1 atm. Theoretical film boiling results for conventional fluids have been extended, on the basis of interfacial instability due to gravity, to include liquefied gases properties, such as low viscosity and small surface tension. In the experiments, primarily ordinary liquid helium I has been studied to extend the range of the film boiling Rayleigh numbers (based upon Laplace's reference length) from about 10^7 (reported for room temperature liquids) to values of the order of magnitude unity. The heat transfer data taken at surface excess temperatures $\triangle T$ (above the boiling point) between 80° and 300°K. have been correlated with a theoretical model which presumes the absence of any scaling length (Laplace length) associated with surface tension. At low $\triangle T$ the experimental results have been found to agree with a model which presumes a negligible influence of a scaling length due to surface tension and absence of detectable viscosity effects.

In low boiling point liquids, film boiling starts at only a few degrees temperature difference between solid and liquid. Therefore, in the cryogenic range of the temperature scale, this boiling mode is encountered quite frequently. Since all liquefied gases down to the λ point of the helium I–helium II transition exhibit ordinary liquid behavior, it should be expected that boiling correlations for room temperature liquids may account for helium I phenomena. This liquid, however, has an extraordinary low surface tension and heat of vaporization at standard pressure. Further, when it is brought in contact with a body at room temperature, the Leidenfrost film formed has a vapor excess enthalpy ratio $c_p\Delta T/\lambda$ which is substantially larger than values from known film boiling experiments with room temperature liquids. Therefore, heat transfer data prediction with known correlations constitutes an extrapolation far beyond the range of property values covered in presently known experiments with conventional liquids. This extrapolation is questionable, in particular, when surface tension is expected to be a governing variable, as for instance during film boiling above a horizontal plate.

Work with horizontal cylinders has been described early by Bromley (*1*), who proposed the first film boiling model which permitted satisfactory correlation of data at quasi-laminar film boiling Rayleigh numbers (*2*). Hsu and Westwater (*3*) studied film boiling on vertical surfaces and found that turbulent film flow may occur already for comparatively short test sections. Film boiling on a horizontal plate has been investigated by Berenson (*4*). He found a regular bubble pattern during boiling of *n*-pentane and CCl_4 above a heat transfer surface which was located at the bottom of a tube. The film boiling Rayleigh number had the order of magnitude 10^6 to 10^7, and the tube diameter was comparable with Laplace's reference length B. Hosler and Westwater (*5*), on the other hand, also used low temperature liquids and extended Berenson's kinematic investigations by conducting optical studies of the bubble pattern above shallow fluid layers of Freon-11 and water on a surface whose area was much larger than B^2. Similar research of the Leidenfrost phenomenon with extended liquid masses has been reported by Patel and Bell (*6*) for water and organic liquids. While doing extended studies of nucleate boiling in helium I, Lyon (*7*) reported a few film boiling data at small ΔT values.

Theoretical investigations have focussed attention upon the heat convection process (*1*). In addition, the process of bubble formation has been considered on the basis of instability results derived in classical isothermal hydrodynamics (*8*). Early applications of the classical theory to film boiling have been proposed by Chang (*9*) and Zuber (*10*). It was Berenson (*4*), however, who, on the basis of his experiments, convincingly showed for the first time that the heat convection approach can be combined with instability results to obtain a complete natural convection two-phase flow model of film boiling which incorporates vapor removal information. He further provided experimental evidence that the instability phenomenon is not restricted to the Leidenfrost point (heat flux minimum), but may be applied to the entire range of film boiling if appropriately modified. The classical stability results, however, do not account for nonisothermal fluids. Therefore, Berenson employed an approximate method and obtained interfacial growth rates at finite temperature differences of real film boiling by inserting the vapor film thickness of the heat convection approach into classical isothermal dispersion relations (see Figure 2 in reference *4*). Subsequent investigations (*5*, *6*) have recognized the potential of the instability approach; however, the experimental results indicated that the model of reference *4* might be a special case. On the large horizontal surfaces of the model in reference *5*, the bubble pattern differed somewhat from the configuration in reference *4*. Further, Zuber (*10*), in his application of instability relations to the heat flux minimum, presumed that the vapor removal process is not affected by viscosity, while the low minimum flux value in reference *4* indicates that viscous effects may be felt with certain configurations.

In view of these uncertainties, the investigations reported in this paper had the following purposes: extension of the presently known theoretical models on the basis of

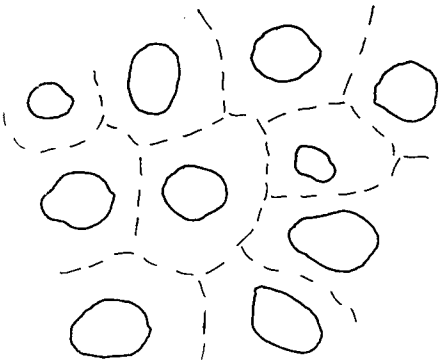

Fig. 1a. Schematic sketch of vapor-liquid interface. Large surface seen from above.

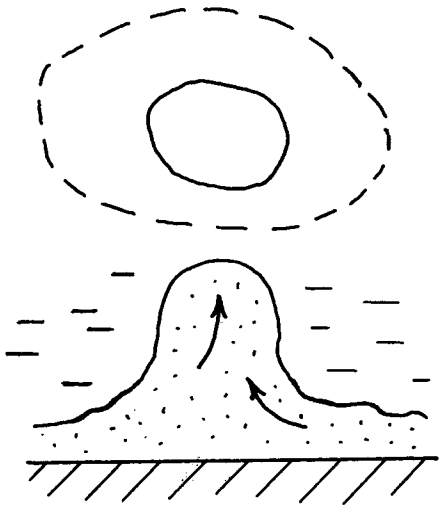

Fig. 1b. Schematic sketch of vapor-liquid interface. Single cell.

instability approaches; experimental studies of helium I down to small film boiling Rayleigh numbers of about unity; comparison of test data with the various models and evaluation of conclusions concerning instability effects upon film boiling. In the beginning, Berenson's approach is extended to take into account the temperature effects on dispersion relations resulting from stability analysis and possibilities of different vapor flow regimes. As a result, new thermohydrodynamic models are obtained. A later section of this paper describes the helium I experiment conducted, which provided quasisteady heat removal rates during application of a transient technique. Finally, conclusions are drawn which are concerned with a better understanding of the various boiling conditions at a horizontal surface and related transitions in boiling mode.

THEORETICAL MODELS

When a liquefied gas is placed above a horizontal surface of a room temperature body, a vapor blanket will be formed due to heat supply from the wall to the liquid. If the time-dependent position of the resulting vapor-liquid interface and the vapor-velocity field were known, the rate at which liquid is converted into vapor could be determined readily. At standard gravity, however, the fluid arrangement (less dense vapor underneath dense liquid) is not the configuration of lowest potential energy, and the system tries to approach minimum energy configurations. This process, in general, causes considerable interfacial motion with a subcooled or saturated liquid. In this section, the latter case will be considered exclusively during steady state conditions. The vapor-liquid interface breaks up when disturbances have such a large size and radius of curvature that the resulting surface forces are not strong enough to oppose the action of gravity. This instability gives rise to bubble formation. During steady state, the amount of vapor carried away with the departing bubbles has to be equal to the amount of vapor produced by the heat supplied from the wall. Accordingly, the subsequent discussion deals separately with these two effects after simplifying assumptions have been made. To account for the thermal effects, a cellular interfacial pattern is introduced. The bubble formation, on the other hand, will be treated on the basis of the classical stability analysis by means of the small perturbation method.

Cellular Pattern

An observer or a camera viewing the horizontal plate from above sees interfacial deformations at certain locations as sketched in Figure 1*a*. The disturbances grow until bubbles are formed and removed. During the next time interval, vapor accumulation takes place somewhere else. This irregularity does not give much hope to arrive at a detailed and rigorous description unless simplifications are made. We assume stochastic properties such that the bubble-size distribution over a sufficiently large surface area at a given time is not significantly different from the observed size distribution at a given surface area element, as a function of a sufficiently long time interval. Then it suffices to consider the vapor production at a given time. In accordance with this assumption only simple distribution functions will be subsequently introduced. A boundary is drawn around each vapor removal site (Figure 1*a*) which defines cells. Each cell is composed of two regions: an outer thin vapor layer near the cell boundary and a thick vapor core near the center of the cell (Figure 1*b*). As soon as the various cell sizes and suitable scaling factors for the film thickness determination are known, the vapor produced may be determined. Because of the as yet unknown cell size, however, we give only approximate details of the cell thermohydrodynamics.

The heat passes most readily across the thin vapor layer outside the cell core and produces a vapor volume flow rate $\dot{V}_1$:

$$\dot{Q} = \dot{V}_1 \rho \lambda' \tag{1}$$

where an effective heat of vaporization, $\lambda' = \lambda + 0.5 c_p \Delta T$ has been used. The thermal impedance of the vapor layer is accounted for by Fourier's law:

$$\dot{Q} \sim L^2 k \Delta T/\delta \tag{2}$$

The scaling factor in this proportionality relation is the cell size L, to be found from instability results. The average rate of vapor production ($\dot{V}_1$) during the lifetime of the cell has to match the volume flow rate $\dot{V}_2$ out of the outer zone to the core. When the vapor superheat does not change significantly during the motion, we have

$$\dot{V}_1 \approx \dot{V}_2 \tag{3}$$

The volume flow rate $\dot{V}_2$ may be expressed in terms of the mean velocity and the cross section available to the flow

$$\dot{V}_2 \sim \bar{v} L \delta \tag{4}$$

Then the relations (1) to (4) yield a film thickness

$$\delta^2 \sim (L k \Delta T)/(\rho \lambda' \bar{v}) \tag{5}$$

and a heat current density

$$q \sim L^{3/2} (k \Delta T \rho \lambda' \bar{v})^{1/2} \tag{6}$$

So far, the lifetime of the cell and its geometry are unknown, in particular v, L, δ. Therefore, we turn now to

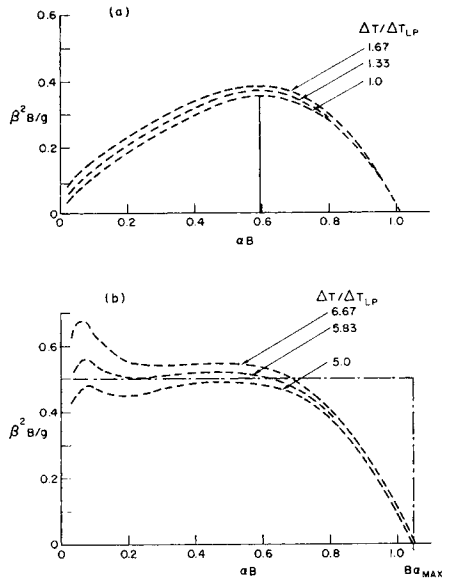

Fig. 2. Growth rate parameter β as a function of wave number. (*a*) Small vapor superheat. (*b*) Large vapor superheat.

the interfacial phenomena which affect cell sizes and growth rates.

Interfacial Breakup and Bubble Growth

A useful tool which elucidates the process of interfacial breakup is the method of small perturbations (*8*). In general, this approach yields dispersion relations which describe the angular frequency ω as a function of wave number α in the range of stable disturbances (capillary waves), including the interfacial growth rates $\beta(\alpha)$ of perturbations at unstable wave numbers. Only the unstable case is significant for our present geometry. When two-dimensional disturbances with amplitudes proportional to $\exp(-i\omega t)$ are superimposed on the horizontal interface between inviscid, isothermal liquid and vapor, there will be a wave number range of imaginary ω values where $\omega = i\beta$ (β real). Growth of the disturbances takes place at a rate

$$\exp(\beta t) = 1 + \beta t \ldots . \qquad (7)$$

When the undisturbed fluids are stagnant (zero translational velocities) the growth or amplification factor β is given by

$$\beta^2 = (g(\rho_L - \rho_v) - \sigma\alpha^2)/(\rho_L \coth \alpha\delta_L + \rho_v \coth \alpha\delta_v) \qquad (8)$$

When the liquid is of finite extent ($\coth \alpha\delta_L \rightarrow 1$) and the vapor layer is thin ($\coth \alpha\delta_v \approx 1/\alpha\delta_v$), Equation (8) reduces to

$$\beta = (\alpha g(\rho_L - \rho_v) - \sigma\alpha^3)^{1/2}/(\rho_L + \rho_v/\delta_v\alpha)^{1/2} \qquad (9)$$

Equation (9) has a maximum growth rate $\beta^*(\alpha^*)$, when $\partial\beta/\partial\alpha = 0$, which is found to be near the wave number $1/(3^{1/2}B)$. Equations (8) and (9), however, do not account for real, nonisothermal film boiling, which poses many difficulties to a rigorous approach. Therefore, temperature effects have been taken into account by means of the approximate method of reference *4*. Results of these calculations have been given in Figure 2 in nondimensional form. We note that only the order of magnitude of $\Delta T/\Delta T_{LP}$ appears to be significant because of the semiempirical approach (*4*) taken and due to lack of experimental β values. Figure 2*a* shows the temperature effects on $\beta(\alpha)$ when ΔT is small. Figure 2*b* gives the amplification function at elevated excess temperatures. At small ΔT there is a well-defined maximum close to the wave number α^* of Equation (9). As ΔT is increased, however, there is no longer a pronounced maximum at a well-defined wave number. On the basis of the flat β characteristics, a wide range in bubble sizes has to be expected.

We have to point out that the final bubble size and bubble removal frequency cannot be predicted *quantitatively* from the dispersion relation because of time restrictions of the analysis and configurational effects. The real growth is nonlinear such that some of the higher order terms in Equation (7) become negative when the range of small perturbations is exceeded. Also, because of real three-dimensional growth, further geometric corrections are required. Consequently, no refinements are made and the subsequent models are formulated on the basis of two simplified amplification functions $\beta(\alpha)$. The functions are expected to represent extreme situations which account qualitatively for most of the phenomena observed in physical reality. In the first case, we replace the amplification spectrum by a single line $\beta^*(\alpha^*)$ from Equation (9). Thus

$$\beta = \beta^* = (2g/B(3)^{3/2})^{1/2}\,[(\rho_L - \rho_v)/\rho_L]^{1/2} \qquad (10)$$

at $\alpha = \alpha^* = 3^{-1/2}\,B^{-1}$

Accordingly, all statistical elements are eliminated from Equation (9) so that one single bubble size and period occurs; in other words, a regular vapor removal pattern results. Numerical values may be worked out readily for this situation (for example, triangles, squares as cellular patterns). The second function represents another extreme and is obtained by substituting for the β characteristics of Figure 2*b* the simple relation

$$\beta = \text{const for } 0 < \alpha < \alpha_{max} \qquad (11)$$

where α_{max} is the cutoff wave number of neutral stability. Accordingly, no predominant bubble size is expected to occur at all, and all sizes are likely to become visible.

Thermohydrodynamic Models

After introduction of the two simplified amplification spectra, the number of extreme possibilities is readily extended to four by considering the two possible modes of vapor motion: stable laminar flow at low Reynolds number, and unstable turbulent motion with inertia forces much larger than the viscous forces (high Reynolds number). Thus, the following four thermohydrodynamic cases result: Model I: Regular cellular two-phase flow [Equation (10)] and laminar vapor flow. Model II: Regular cellular two-phase flow [Equation (10)] and vapor flow dominated by inertia forces. Model III: Vapor removal at random [Equation (11)] and laminar vapor flow. Model IV: Vapor removal at random [Equation (11)] and vapor flow dominated by inertia effects.

Since the four models describe quite extreme possibilities, we expect to have sufficient coverage of experimentally realizable situations.

Model I. In accordance with Equation (1), this case is dominated by a constant cell size ($L \sim B$). Thus, L, as well as the height of the vapor core, is proportional to B. Consequently, the driving gravitational pressure difference $\Delta p = g(\rho_L - \rho)L$ also will be proportional to B. The previous dimensional relations are extended readily to laminar flow of vapor which has a mean velocity proportional to Δp. Then

$$\bar{v} \sim \delta^2\,\Delta p/\mu\,L \sim g(\rho_L - \rho)\,\delta^2/\mu \qquad (12)$$

the film thickness becomes

$$\delta \sim (k\,\mu\,L\,\Delta T/g\,\rho(\rho_L - \rho)\,\lambda')^{1/4} \qquad (13)$$

where $L \sim B$, and the heat current density turns out to be

$$q \sim (k^3\,\Delta T^3\,g\,\rho(\rho_L - \rho)\,\lambda'/\mu\,L)^{1/4};\quad L \sim B \qquad (14)$$

This result may be written in a dimensionless form. The nondimensional heat transport number (Nusselt number)

may be expressed in terms of the Rayleigh number, $N_{Ra} = B^3 g \rho(\rho_L - \rho)c_p/\mu k$, which contains the reference length B.

$$N_{Nu} = C_1 (N_{Ra} \lambda'/c_p \Delta T)^{1/4} \quad (15)$$

This model has been proposed by Berenson (*4*), who correlated his experimental data of room temperature liquids by means of $C_1 = 0.425$. In accordance with Equation (10), he observed regular kinematic conditions, since the surface area was small (diameter of the order of magnitude B). In addition, viscous retardation of fluid motion could take place readily, since vertical walls surrounded the small heat transfer surface.

Model II. We retain the Equation (10) and the regular array of vapor release points. However, we presume that the inertia forces overrun the viscous forces at high Reynolds numbers. Then

$$\bar{v} \sim (\Delta p/\rho)^{1/2} \sim (g(\rho_L - \rho)\ L/\rho)^{1/2};\ L \sim B \quad (16)$$

and the film thickness becomes

$$\delta \sim (k \Delta T/\lambda')^{1/2} (L/g\ (\rho_L - \rho)^{1/4};\ L \sim B \quad (17)$$

This yields a heat current density of

$$q \sim (k \Delta T \lambda')^{1/2} (g\ (\rho_L - \rho)/L)^{1/4}\ ;\ L \sim B \quad (18)$$

This thermal result may be formulated in dimensionless form as

$$N_{Nu} = C_2 (N_{Ra} N_{Pr} (\lambda' c_p \Delta T)^2)^{1/4} \quad (19)$$

Inviscid flow has been suggested by Kistemaker (*11*) to account for the behavior of subcooled liquid in the Leidenfrost state. His situation, therefore, is thermally and hydrodynamically different from our saturated liquid model.

Model III. When bubbles are formed and removed completely at random and the size varies arbitrarily within the range given by Equation (11), there will be no predominant bubble dimension. Equations (12) and (13) do apply; however, the L values are distributed at random. Consequently, on a large surface whose area exceeds B^2 considerably, it is not possible to have an effect of any length on the heat transport when Equation (11) is valid. To determine the governing heat transport relation, we use dimensional reasoning and consider the function $N_{Nu} = N_{Nu} (N_{Ra} \lambda'/c_p \Delta T)^m$. The only value of the exponent m which fulfills Equation (3) is $m = 1/3$. Then, any length effect disappears. The heat flow density becomes

$$q = C_3 (k \Delta T)^{2/3} [g (\rho_L - \rho) \rho \lambda'/\mu]^{1/3} \quad (20)$$

in accordance with the dimensionless equation

$$N_{Nu} = C_3 (N_{Ra} \lambda'/c_p \Delta T)^{1/3} \quad (21)$$

We may insert in Equation (21) any reference length which is convenient, for instance, B. This formalism, however, does not imply that the heat transport would depend on surface tension. An equation of this kind has been suggested by Chang (*5*), who arrived at $C_3 = 0.294$ without referring explicitly to condition (11).

Model IV. When the inertia forces dominate and vapor is removed at random, neither the viscosity nor the surface tension are significant variables so far as the heat transport is concerned. The details are worked out in the same way as before and we obtain a Nusselt number

$$N_{Nu} = C_4 (N_{Ra} N_{Pr})^{1/3} (\lambda'/c_p \Delta T)^{2/3} \quad (22)$$

and

$$q = C_4 (k \Delta T\ g\ (\rho_L - \rho)/\rho)^{1/3} (\rho \lambda')^{2/3} \quad (23)$$

In view of the small surface tension of helium I and other extreme property values, the physical significance of the models should be discovered readily from helium I test data. Before turning to the experiment, however, we add the remark that pure, single-phase heat transport due to gravity action may be approached along *exactly* the same line of thought. Then, $\lambda \to 0$, $\lambda' \to$ const., and $N_{Ra} \lambda'/c_p \to$ const. N_{Ra}. In particular, when $\Delta T << T$, the density difference may be conveniently expressed in terms of the temperature difference by using the isobaric coefficient of thermal expansion. The film boiling Rayleigh number then becomes the product of the single-phase Grashof and Prandtl number, which is the special case referred to in most heat transfer texts.

EXPERIMENTAL INVESTIGATIONS

The experiments were conducted in a helium cryostat at a pressure of 1 atm. with thermocouple thermometry which covered the range from room temperature to about liquid nitrogen temperatures. The test assembly was somewhat similar to the specimen employed by Challis (*12*) for Kapitza resistance measurements. A number of modifications, however, avoided a complex heat leak evaluation. The experimental apparatus (*H 20* in Figure *3a*) contained a horizontal surface as heat transfer area which was the upper end of a vertical cylinder (*A*) out of electrolytic tough pitch, annealed copper (0.187 in. wide, 0.150 in. long). This cylinder was used as a calorimetric device. Vacuum insulation provided an adiabatic enclosure and separated the specimen from the surrounding liquid bath. To reduce radial temperature gradients and resulting radial heat currents, a guard ring (*B*) surrounded the copper cylinder so that the heat transfer surface proper

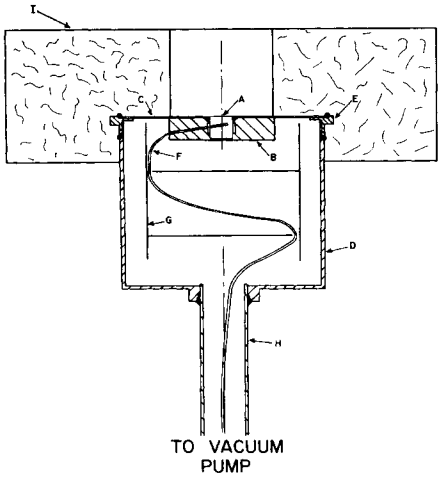

Fig. 3*a*. Vacuum-insulated specimen *H 20* (overall diameter of Styrofoam block 2.9 in.; guard ring O.D. 0.75 in.).

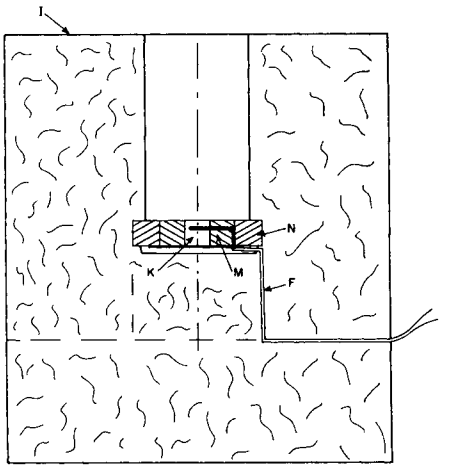

Fig. 3*b*. Styrofoam-insulated specimen *H 19* (overall diameter 2.8 in.; height 3.2 in.; diameter of guard ring N:0.94 in.).

was about 0.002 in. above the ring. A brass ring was first used and later was replaced by a copper one. The cylinder was attached by silver soldering to the guard ring and soldered to a piece (C) of shimstock of stainless steel 304 (1 mil) with a center hole cut for the cylinder. At the outer circumference, the stainess steel foil was connected by silver soldering to a ring (E) which, for easy separations, had a soft solder joint with the vacuum case (D). Final machining of the central joints produced a smooth horizontal copper test surface. One copper-constantan thermocouple (F) was attached to the central cylinder by means of Woods metal after preliminary runs with two thermocouples near both ends had shown only small temperature differences of about 1.5°K. within the copper. The thermocouple wires, after passing a radiation shield (G) out of 1 mil copper shimstock, were kept inside the vacuum tube (H) and were taken out of the vacuum system at room temperature by means of Kovar feed-throughs. A Honeywell-Brown potentiometric strip chart recorder displayed the temperatures as a function of time.

The assembly out of metallic parts described so far had serious heat leaks. Experiment and computation showed that up to 50% of the heat crossing the test area was removed through the stainless steel foil (C). This high value was caused by liquid-foil contact, and, unfortunately, could not be accounted for by a simple correction method, since the vapor–liquid–solid contact line moved during the experiment. Consequently, the foil (C) and the outer region near the ring (E) were covered by a Styrofoam block (I). The resulting radial heat flow through the foil was calculated to be less than 3% of the total heat flow to the liquid.

The tube (H) was connected to a vacuum pumping system (mechanical forepump and diffusion pump) by means of a flexible hose which permitted vertical motion of the assembly for immersion into and removal out of the liquid bath. The cryostat consisted of two conventional glass dewars. The inner silvered helium dewar had a strip window for observations, an inner diameter of about 3 in., and a height of about 4 ft. After immersion of the assembly in the liquid helium, transient cool-down took place with quasi steady heat removal in the film boiling regime. This transient technique has the advantage of reducing the liquid helium consumption considerably so that the most efficient use is made of a given amount of liquid. The reliability of this method has been demonstrated by several investigators (*13, 14*) whose data showed good agreement with steady state results. Additional nitrogen runs were conducted, in particular during the preliminary period of specimen checkout and improvement. In general, the nitrogen runs showed greater scatter of data than the helium experiments. The data were reduced and evaluated in the same way as in cylinder investigations (*15*).

A number of preliminary studies employed simple Styrofoam-insulated specimens, such as sample *H 19* of Figure *3b*. Styrofoam may be used conveniently for many purposes as described, for instance, in reference *16*. This simple type of insulation is very attractive, not only for the present studies. Detailed investigations showed that the helium data obtained from specimen with proper Styrofoam insulation agree well with results from vacuum insulated assemblies. The nitrogen tests again showed greater scatter than the helium I studies. We note that at liquid helium or hydrogen temperatures, a large percentage of the interstitial gases in the Styrofoam pores is condensed. Thermometry and inner copper cylinder (K) (0.192 in. diameter, 0.192 in. long) did not deviate in principle from the specimen *H 20*. The thermal properties of the brass rings (M) and (N) around the cylinder deviated slightly from the copper values; however, the error is not larger than the scatter of experimental data encountered in the tests. The helium I results from both specimens agree well; therefore, we conclude that it is possible to obtain good insulation by means of Styrofoam even at large ΔT values.

DATA DISCUSSION AND COMPARISON WITH THEORY

The helium I heat transfer coefficients have been plotted in Figure 4.† They show the order of magnitude

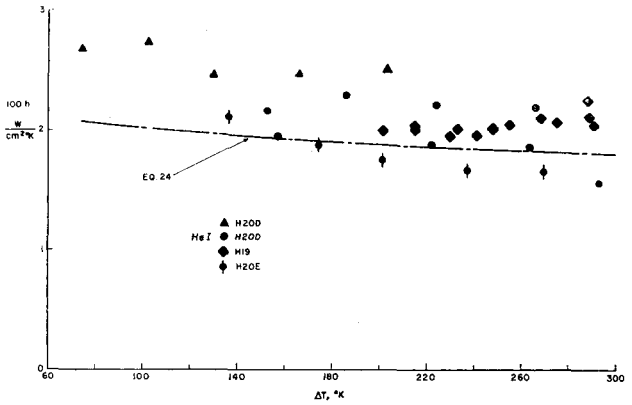

Fig. 4. Helium I heat transfer coefficients as a function of ΔT.

which is typical of the Leidenfrost phenomenon or film boiling. We note that visual inspection did not show any regular vapor removal pattern. To obtain insight into the physical significance of the models, the data were plotted first as reduced heat flow densities vs. ΔT where a reference q value was used. These plots indicated, in particular for nitrogen, that the ΔT-dependence is represented by either model III or IV. Consequently, limited support appeared to be available for models I and II. Since model I, however, has been applied successfully in room temperature liquid investigations (*4*), the data have been plotted in dimensionless form as N_{Nu} vs. $N_{Ra}\,\lambda'/c_p\Delta T$ in Figure 5.

Figure 5 shows the film boiling Rayleigh number range covered in the present helium I experiments and previous investigations with conventional fluids. This plot of N_{Nu} vs. $N_{Ra}\,\lambda'/c_p\Delta T$ is particularly convenient for a comparison of model I with III. Our helium I Nusselt numbers are lower than Berenson's prediction (model I). This difference might possibly be caused by the fact that his correlation was based upon experiments with room temperature liquids for a comparatively small surface. In Figure 5, we have included helium I results by Lyon (*7*), who investigated the range of small ΔT values by means of carbon resistor thermometry. His data deviate somewhat from the correlation suggested by model III and indicate that the heat flow resistance might be reduced near the heat flux minimum. This deviation is similar to the nitrogen behavior found in our experiments near the Leidenfrost point and suggests a predominance of inertia effects.

When less weight is assigned to the low vapor superheat data of helium and nitrogen, model III seems to pro-

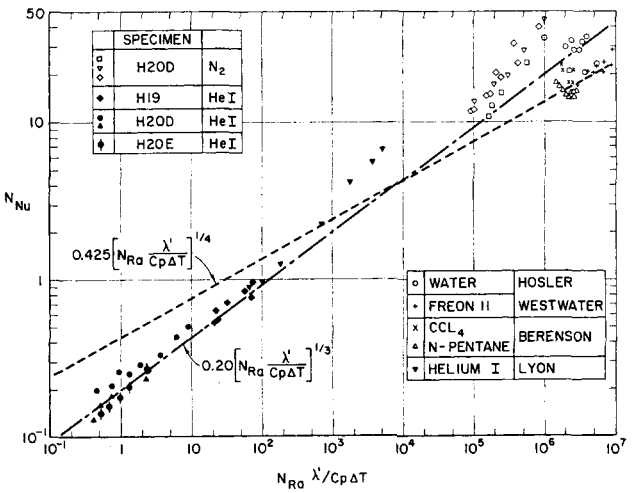

Fig. 5. Nusselt number as a function of the film boiling Rayleigh number.

† Complete data have been deposited as document 8649 with the American Documentation Institute, Photoduplication Service, Library of Congress, Washington 25, D. C., and may be obtained for $1.25 for photoprints or 35-mm. microfilm.

vide a fair representation of film boiling heat transfer of cryogenic liquids and some of the room temperature data on extended surfaces (5). We have, therefore, correlated these data by means of

$$N_{Nu} = 0.20\ (N_{Ra}\,\lambda'/c_p\Delta T)^{1/3} \qquad (24)$$

with physical properties evaluated at the arithmetic mean film temperature between the hot wall and the liquid. The excess enthalpy λ' has been inserted since other effective latent heat expressions will be in error for helium I (15) at high vapor superheat.

At low vapor superheat, model IV has also been found to be useful for the cryogenic liquids helium I and nitrogen. The data could be correlated fairly well with

$$N_{Nu} = 0.30\ [N_{Ra}\ (\lambda'/c_p\Delta T)^2\, N_{Pr}]^{1/3} \qquad (25)$$

Additional data taken by Lyon (7) near the λ and critical point agreed with the 1 atm. results, but have been omitted because of property uncertainties. There are, however, serious deficiencies in Equation (25) so far as room temperature liquids are concerned, whose heat transfer is overestimated considerably. To explain the discrepancy, it is assumed that the viscous effects play a significant role when the viscosity is large at elevated temperatures, and inertia effects apparently dominate at low temperatures when the viscosity is small. For the purposes of comparison, other helium I film boiling data have been included in Figure 6 and, in addition, a few nucleate boiling results for liquid temperatures in the range $T_\lambda < T <$ 2.3°K. reported by Karagounis (17), Lyon (7), and Madsen (18).

According to the present investigations, the film boiling of liquefied gases differs from the kinematic regularity encountered with conventional fluids at small surfaces (4). The gradual transition of helium I film boiling from correlation (24) of model III at large ΔT values to the correlation (25) of model IV at small ΔT indicates that intermediate phenomena may be found between the limiting possibilities of the models. This behavior appears to be supported also by the investigations on comparatively large surfaces in references 5 and 6. Accordingly, there is no single-valued minimum flux q_{LP}, and the special conditions of each configuration have to be taken into account. By imposing forced convection, obviously *any* q_{LP} value could be found beyond the lower bounds specified by model I [Equation (15)], model III [Equation (24)], or model IV [Equation (25)]. This possibility eliminates the prediction of the Leidenfrost point and the related minimum excess temperature difference ΔT_{LP} of film boiling by means of purely hydrodynamic reasoning. Therefore, more general criteria appear to be relevant, and use may be made of the thermodynamic metastability limit which seems to be the only criterion left. To estimate q_{LP} in a particular situation, we may insert the maximum metastable superheat ΔT_{max} into one of the appropriate correlations. For instance, in case of model III we have

$$q_{LP} \approx 0.2\ (k\,\Delta T_{max})^{2/3}\ [g\ (\rho_L - \rho)\ \rho\,\lambda'/\mu]^{1/3} \qquad (26)$$

Since no detailed values of the maximum metastable liquid superheat are known as yet, we may insert, for crude estimates, roughly two times the average nucleate boiling superheat ΔT_{LP} given in reference 19.

CONCLUSIONS

We draw the following conclusions from the present investigations:

1. Surface tension is unimportant so far as film boiling heat transport to cryogenic liquids from large surfaces is concerned.

2. Irregular kinematic conditions prevail at large surfaces and large temperature differences; therefore, all relations based on kinematic regularity, such as minimum flux relations and bubble frequency-diameter functions, are special results.

3. The two simple models, III and IV, constitute limits to film boiling heat transfer of liquefied gases on large horizontal surfaces subjected to gravitational instability, and are lower bounds to the related forced convection two-phase flow at solid wall excess temperatures beyond the liquid metastability limit.

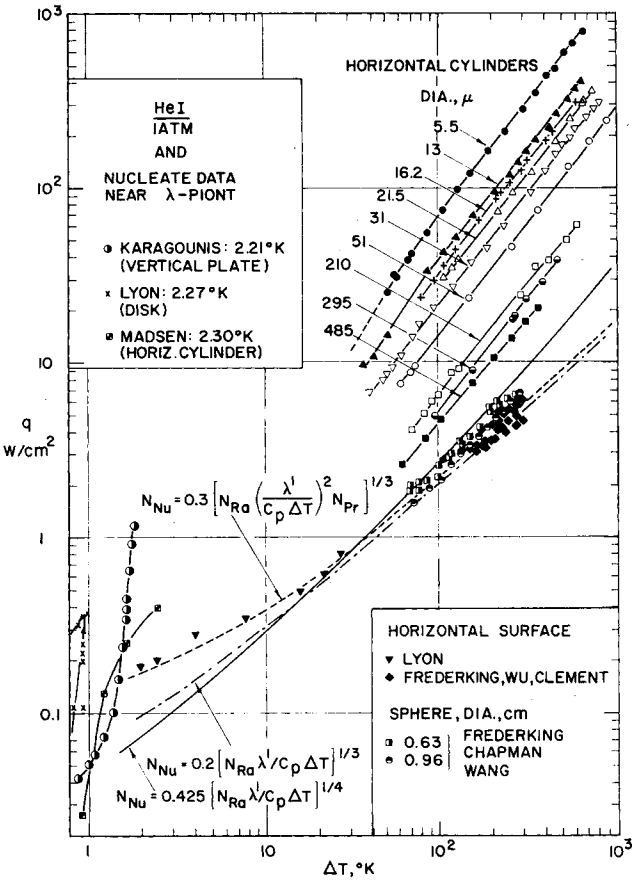

Fig. 6. Helium I heat flux densities as a function of ΔT.

ACKNOWLEDGMENT

Part of this research has been supported by the National Science Foundation under Grant GP-1889.

NOTATION

Properties without subscript to be evaluated at arithmetic mean vapor film temperature.

B = Laplace's reference length, $(\sigma/(\rho_L - \rho_v)g)^{1/2}$
C_1, C_2, C_3, C_4 = constants
c_p = specific heat
g = acceleration due to gravity
k = thermal conductivity
L = reference length
N_{Nu} = Nusselt number (containing reference length L)
Δp = pressure difference
N_{Pr} = Prandtl number
Q = heat current
q = heat current density
N_{Ra} = Rayleigh number $= B^3 g\,\rho\,c_p(\rho_L - \rho)/k\,\mu$
ΔT = temperature difference between wall and saturation value
$\bar{v}$ = mean velocity
$\dot{V}_1$ = vapor volume production per unit time
$\dot{V}_2$ = vapor volume flow rate

Greek Letters

α = wave number
β = amplification factor
δ = vapor film thickness
λ = heat of vaporization
λ' = $\lambda + 0.5\ c_p\ \Delta T$
μ = dynamic viscosity
ρ = density
σ = surface tension
ω = angular frequency

Subscripts

LP = Leidenfrost point (q minimum)
L = saturated liquid
v = saturated vapor
max = maximum

LITERATURE CITED

1. Bromley, L. A., *Chem. Eng. Progr.*, **46**, 221 (1950).
2. Frederking, T. H. K., and J. A. Clark, *Advan. Cryog. Eng.*, **8**, 501 (1963).
3. Hsu, Y. Y., and J. W. Westwater, *A.I.Ch.E. J.*, **4**, 58 (1958).
4. Berenson, P. J., *J. Heat Transfer*, **83C**, 351 (1961).
5. Hosler, E. R., and J. W. Westwater, *A.R.S. J.*, **32**, 553 (1962).
6. Patel, B. M., and K. J. Bell, paper presented at A.I.Ch.E. Los Angeles meeting (August, 1965).
7. Lyon, D. N., *Intern. Advan. Cryog. Eng.*, **10**, 371 (1965).
8. Lamb, H., "Hydrodynamics," p. 455, Dover, New York (1945).
9. Chang, Y. P., *J. Heat Transfer*, **81C**, 1 (1959).
10. Zuber, N., *Trans. Am. Soc. Mech. Engrs.*, **80**, (1958); Ph.D. thesis, Univ. California, Los Angeles (1959).
11. Kistemaker, T., *Physica*, **29**, 351 (1963).
12. Challis, L. J., *Proc. VII, Intern. Conf. Low Temp. Physics*, Toronto, 476 (1960).
13. Ruzicka, J., "Heat Transfer to Boiling Nitrogen", "Problems of Low-Temperature Physics and Thermodynamics," p. 323, Pergamon Press, New York (1959).
14. Merte, H., Jr., and J. A. Clark, *Am. Soc. Mech. Engrs. Paper No. 63-HT-28.*
15. Frederking, T. H. K., *J. Appl. Math. Phys.*, **14**, 207 (1963).
16. Marshall, L., *Rev. Sci. Instruments*, **26**, 614 (1955).
17. Karagounis, A., *Suppl. Bull. Inst. Intern. Froid*, Annex 2 (1956).
18. Madsen, R. A., Ph.D. thesis, p. 78, Purdue Univ., Lafayette, Ind. (1965).
19. Frederking, T. H. K., *Advan. Cryog. Eng.*, **9**, 71 (1964).

Manuscript received March 9, 1965; revision received September 28, 1965; paper accepted October 1, 1965 Paper presented at A.I.Ch.E. San Francisco meeting.

Why Thermodynamics Is a Logical Consequence of Information Theory

MYRON TRIBUS, PAUL T. SHANNON, and ROBERT B. EVANS

Dartmouth College, Hanover, New Hampshire

An observation of the properties of bulk matter necessarily omits many details of the motion of the particles which comprise that matter. If a communication regarding the observation is to be consistent, it must conform to certain rules which follow from the theory of information. An analysis of the problem of deciding upon a consistent encoding for such observations leads, as a unique result, to the concepts and equations of classical thermodynamics. The information-theory analysis of this problem also leads to a better understanding of the basis for the "laws" of thermodynamics.

Consider an observer who wishes to report as faithfully as he can his observations of his environment. If he has any experience at all, he is aware that his observations are seldom accurate or complete. At the very minimum he realizes that his knowledge is tentative, that is, not so much subject to correction (as when one misinterprets a 7 for a 1), but rather subject to reinterpretation (as when it is found that the 1 is part of a binary, not a decimal system). The observer sends his observations to a receiver and, if the messages sent to the receiver are to carry the